Bioorganic & Medicinal Chemistry 25 (2017) 5238–5246

Contents lists available at ScienceDirect

Bioorganic & Medicinal Chemistry

journal homepage: www.elsevier.com/locate/bmc

Chemoselective fluorination and chemoinformatic analysis of griseofulvin: Natural vs fluorinated fungal metabolites

Noemi D. Paguigan [a], Mohammed H. Al-Huniti [a], Huzefa A. Raja [a], Austin Czarnecki [b], Joanna E. Burdette [b], Mariana González-Medina [c], José L. Medina-Franco [c], Stephen J. Polyak [d,e,f], Cedric J. Pearce [g], Mitchell P. Croatt [a], Nicholas H. Oberlies [a,*]

[a] Department of Chemistry and Biochemistry, University of North Carolina at Greensboro, Greensboro, NC 27402, USA
[b] Department of Medicinal Chemistry and Pharmacognosy, University of Illinois at Chicago, Chicago, IL 60612, USA
[c] Department of Pharmacy, School of Chemistry, Universidad Nacional Autónoma de México, Avenida Universidad 3000, Mexico City 04510, Mexico
[d] Department of Laboratory Medicine, University of Washington, Seattle, WA 98195, USA
[e] Department of Global Health, University of Washington, Seattle, WA 98104, USA
[f] Department of Microbiology, University of Washington, Seattle, WA 98195, USA
[g] Mycosynthetix Inc., 505 Meadowlands Drive, Suite 103, Hillsborough, NC 27278, USA

ARTICLE INFO

Article history:
Received 13 June 2017
Revised 19 July 2017
Accepted 24 July 2017
Available online 28 July 2017

Keywords:
Griseofulvin
Xylaria cubensis
Fluorination
Selectfluor
Cytotoxicity
Antifungal

ABSTRACT

Griseofulvin is a fungal metabolite and antifungal drug used for the treatment of dermatophytosis in both humans and animals. Recently, griseofulvin and its analogues have attracted renewed attention due to reports of their potential anticancer effects. In this study griseofulvin (**1**) and related analogues (**2**–**6**, with **4** being new to literature) were isolated from *Xylaria cubensis*. Six fluorinated analogues (**7**–**12**) were synthesized, each in a single step using the isolated natural products and Selectfluor, so as to examine the effects of fluorine incorporation on the bioactivities of this structural class. The isolated and synthesized compounds were screened for activity against a panel of cancer cell lines (MDA-MB-435, MDA-MB-231, OVCAR3, and Huh7.5.1) and for antifungal activity against *Microsporum gypseum*. A comparison of the chemical space occupied by the natural and fluorinated analogues was carried out by using principal component analysis, documenting that the isolated and fluorinated analogues occupy complementary regions of chemical space. However, the most active compounds, including two fluorinated derivatives, were centered around the chemical space that was occupied by the parent compound, griseofulvin, suggesting that modifications must preserve certain attributes of griseofulvin to conserve its activity.

1. Introduction

Bioactive secondary metabolites have had a long history in medicine, as they provide privileged scaffolds for drug discovery.[1–4] As testament to this, from 1981 to 2014 over half of the new small molecule drugs approved by the U.S. FDA were natural products or natural product-derived/natural product-inspired.[5,6] The success of natural products as source of therapeutic agents is driven by their biochemical specificity and high chemical diversity, occupying distinct regions of chemical space that coincide with clinically relevant areas.[2,7]

Fungi are one of the most species-rich organisms, second only to insects, offering a vast resource for discovery of new drug leads. Our recent collaborative efforts underscore the structural complexity and diversity of fungal metabolites.[7–9] As promising compounds are identified, these structural features are of particular relevance, as they can be used to stimulate semi-synthetic[10,11] approaches to explore structure-activity relationships and produce new drug candidates.

The natural product griseofulvin (**1**, Fig. 1), (2*S*,6′*R*)-7-chloro-2′,4,6-trimethoxy-6′-methyl-3*H*-spiro[benzofuran-2,1′-cyclohexan]-2′-ene-3,4′-dione, is a potent antifungal drug orally administered for the treatment of dermatophytosis (i.e., fungal infection of the skin) in both humans and animals.[12–15] Since its isolation and discovery from a filamentous fungus in 1939,[16] most research has focused on the identification of griseofulvin analogues, either from nature or synthetically, but to date, only the original compound (**1**) has been developed into a marketable antifungal drug, first approved in 1959.[13] Recently, there has been a renewed interest in **1** due to its antimitotic and antiproliferative activities against various types of cancer cells.[17–21] Griseofulvin has a mode of action

* Corresponding author.
E-mail address: nicholas_oberlies@uncg.edu (N.H. Oberlies).

http://dx.doi.org/10.1016/j.bmc.2017.07.041
0968-0896/

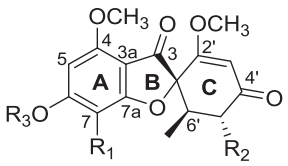

	R_1	R_2	R_3
1	Cl	H	CH_3
2	Cl	OH	CH_3
3	H	H	CH_3
4	H	OH	CH_3
5	H	H	H
6	Cl	H	H

Fig. 1. Structures of griseofulvin (**1**) and related analogues (**2**–**6**) isolated from *Xylaria cubensis* (strain MSX48662).

that is still not well understood, but disruption of the microtubule dynamics in both fungal and mammalian cells has been proposed.[13,22,23] Thus, aside from being an antifungal drug, it may also be a clinically-viable candidate for cancer chemotherapy.[21–26] Due to these reasons, it was decided that the isolation and semi-synthesis of griseofulvin analogues was worth further investigation.

The introduction of fluorine into a bioactive compound has been shown to impart a range of effects, often altering physicochemical profiles by modulating acid/base properties, electronegativity, lipophilicity, and metabolic stability.[27,28] Focusing on these unique properties, fluorine has been exploited in the design and optimization of biologically active molecules.[27,29,30] With our interest in late stage fluorination of secondary metabolites,[10] we envisioned the ability to prepare various fluorinated griseofulvin derivatives. Our approach hinged on the chemoselective nature of Selectfluor as an electrophilic fluorinating reagent. Since the starting materials were the isolated fungal metabolites, it was essential to limit any side reactions of the vinyl ether or epimerization of the asymmetric centers. We further rationalized that **1**, already proven to be a successful therapeutic, was a good candidate to investigate the influence of fluorine substitution as a strategy to expand the medicinally-relevant chemical space of fungal metabolites.

An isolate of the filamentous fungus *Xylaria cubensis* (strain MSX48662) was found to be a prolific producer of **1**, biosynthesizing over 100 mg per a single rice-based fermentation culture grown in a 2.8 L Fernbach flask,[31] and thus, it was used for resupply purposes. Hence, the fungal extract was subjected to further studies and afforded six compounds, including **1** and structurally related analogues, four of which were known (**2**, **3**, **5**, and **6**) and one of which (**4**) was new to the literature. Seven additional fluorinated analogues (**7**, **8a**/**8b**, **9**–**12**) were synthesized using **1**, **3** and **4** as starting materials. All 12 compounds were evaluated for cytotoxicity against cancer cell lines, including human melanoma cancer cells (MDA-MB-435), human breast cancer cells (MDA-MB-231), human ovarian cancer cells (OVCAR3), and human hepatoma (Huh7.5.1) cells.[32] Moreover, the antifungal potency of **1**–**12** against *Microsporum gypseum* was assessed in a disk diffusion assay. Characterization of the chemical space of the isolated and synthesized analogues was also carried out by principal component analysis to correlate structural modifications with the observed bioactivities.

2. Results and discussion

2.1. Isolation of griseofulvin (*1*) and related analogues (*2*–*6*)

Organic extracts ($CHCl_3/CH_3OH$) from the rice-based fermentation cultures of MSX48662 were partitioned with organic solvents, subjected to flash chromatography, and were purified using preparative HPLC to yield griseofulvin (**1**) and five structurally related analogues (**2**–**6**), with **4** being new to literature. The structures of compounds **1**–**3** and **5**–**6** were established by analysis of HRESIMS and NMR data, all of which compared favorably to the literature (See the Supporting Information for spectral data).[33,34]

Compound **4** was isolated as a white solid. The NMR and HRESIMS data (*m*/*z* 335.1119 $[M+H]^+$) both indicated a molecular formula of $C_{17}H_{18}O_7$, corresponding to a difference of an additional OH (16 Da) relative to **3**. The ^1H NMR spectrum of **4** (Table S5 and Figs. S4–S6) showed similarities to **3**, including signals for a 1,2,3,5-tetrasubstituted aromatic ring, as evidenced by the *meta*-coupled aromatic proton signals at δ_H 6.06 and δ_H 6.22 ($^3J_{HH}$ = 1.1 - Hz), an isolated olefinic proton, three methoxy groups, as well as a methyl group. However, it was also clear from these data that the diastereotopic methylene proton α-H-5′ in **3** was replaced with a hydroxy moiety in **4**, thus shifting β-H-5′ to the more downfield region of the spectrum (δ_H 4.71). The large coupling constant ($^3J_{HH}$ = 12.1 Hz) observed between H-5′ and H-6′ placed both protons in *trans*-diaxial positions, imparting 5′-OH and 6′-CH_3 in equatorial positions, analogous to that of **2**. Based on these observations, the configuration at C-5′ was established as *R*. A comparison of the observed specific rotation value ($[\alpha]_D^{27}$ +343) of **4** with those for **1** ($[\alpha]_D^{27}$ +340), **2** ($[\alpha]_D^{27}$ +306) and **3** ($[\alpha]_D^{27}$ +386) revealed that the configurations at C-2 (*S*) and C-6′ (*R*) of these compounds were identical. Thus, the structure of compound **4** was established as shown (Fig. 1) and identified as (2*S*,5′*R*,6′*R*)-7-dechloro-5′-hydroxygriseofulvin.

2.2. Semi-synthesis and structural elucidation of fluorinated analogues

There are a few reports on the fluorination of griseofulvin and its analogues.[35,36] For example, monofluorinated and difluorinated griseofulvin analogues have been prepared by Taub and co-workers in 1963 and Barton and co-workers in 1972 by electrophilic fluorination of griseofulvin using either perchloryl fluoride ($FClO_3$)[37,38] or fluoroxytrifluoromethane (CF_3OF),[39] two of the earliest electrophilic fluorination reagents. These harsh conditions resulted in the formation of several mono- and difluorinated products, including reaction of the enol-ether and some *gem*-difluoro derivatives. Our goal was to chemoselectively fluorinate ring A of griseofulvin without affecting the other functional groups, especially the enol-ether motif. Thus, Selectfluor, was used as the electrophilic fluorination reagent, since it is known to be milder and typically more chemoselective than other fluorination reagents.[40–42] Indeed, this strategy yielded only ring A fluorinated-derivatives; each substrate gave two mono-fluorinated compounds, with fluorination at either C-5 or C-7, which allowed us to probe the chemical space of these analogues.

Seven fluorinated products (**7**, **8a**/**8b**, **9**–**12**) were obtained from Selectfluor reactions with compounds **1**, **3**, and **4** (Scheme 1). Fluorination of compounds **2**, **5**, and **6** was not attempted due to paucity of isolated starting materials from the fungal cultures. Selectfluor was chosen as the electrophilic fluorinating reagent and our results exemplify the chemoselectivity of this reagent. Of the possible reaction pathways, this reagent only fluorinated the C5 or C7 positions. All of the semi-synthetic products could be theoretically synthesized using traditional total synthesis efforts, however, our approach generated at least two completed analogues per reaction using the isolated compounds as the starting materials.

Addition of a solution of **1** (dissolved in CH_3CN) to a CH_3CN solution of Selectfluor afforded one minor compound (**7**) and an inseparable diastereoisomeric mixture of **8a**/**8b** with a ratio of 2:1, as revealed by interpretation of the ^1H NMR data (Fig. S14). The HRMS data for **7** indicated the incorporation of one fluorine atom with a molecular formula of $C_{17}H_{16}ClFO_6$. A comparison of the ^1H NMR data (Table S8, Fig. S9) of **7** with **1** suggested the attachment of a fluorine atom into ring A, as evidenced by the absence of the aromatic H-5 signal. In addition, the methoxy

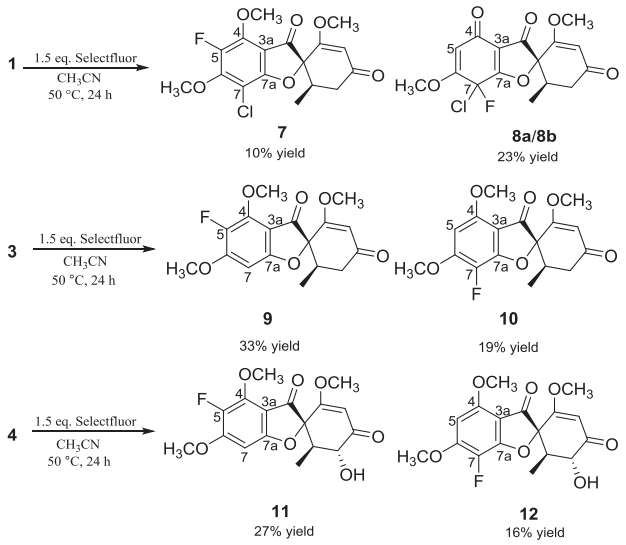

Scheme 1. Semi-synthesis of fluorinated compounds **7**–**12** with Selectfluor. The percent yields were calculated based on isolated product.

groups at C-4 and C-6 resonated as doublets due to through-space coupling[43] with a coupling constant of J_{HF} = 3.1 Hz for both. Their chemical shifts were slightly downfield ($\Delta\delta$ 0.14–0.22, Fig. S10) due to their proximity to the F atom at C-5. ^{19}F–^{13}C HMQC data (Fig. S11) showed a correlation between the fluorine atom and C-5, which resonated as a doublet at δ_C 142.9 with a large coupling constant of 244.3 Hz typical of a $^1J_{CF}$ bond in an aromatic ring,[44] further supporting the position of fluorine. Additionally, the doublet signals observed for C-4 ($^2J_{CF}$ = 9.0 Hz) and C-6 ($^2J_{CF}$ = 12.1 Hz) corroborate the attachment of fluorine at C-5. Altogether, these data identify **7** as 5-fluorogriseofulvin, which was previously reported by Barton and co-workers by the treatment of griseofulvin with fluoroxytrifluoromethane.[36]

The NMR and HRESIMS data (*m*/*z* 357.0543 [M+H]$^+$) for compounds **8a**/**8b** supported a molecular formula of $C_{16}H_{14}ClFO_6$. Following the interpretation of edited-HSQC (Fig. S15) and HMBC (Fig. S16) experiments, the ^{13}C and ^{1}H NMR data (Table S9) were assignable to 16 carbon atoms consisting of two methoxy groups, one methyl, three methine (two sp^2 and one sp^3), one methylene, and nine non-protonated carbons (three carbonyls, four olefinic with three of them oxygenated, and two fully substituted carbons). Comparison of the NMR data between **1** and **8a**/**8b** indicated that rings B and C of both compounds were identical. However, modifications were made in ring A of **8a**/**8b**, as the NMR data indicated oxidation at C-4 to a ketone due to the absence of a methoxy group and the presence of an extra carbonyl carbon (δ_C 176.9). The doublet signal observed for H-5 ($^3J_{HF}$ = 1.8 Hz) and the doublet signal observed for ^{19}F ($^3J_{HF}$ = 1.8 Hz) indicated the addition of fluorine to ring A (Fig. S17). The doublet signal ($^1J_{CF}$ ~253 Hz) observed for C-7, along with an HMQC correlation between ^{19}F and C-7 (δ_C ~94), suggested the attachment of fluorine to C-7 (Fig. S18). The assignment of fluorine being at C-7 was further supported by the doublet splitting patterns observed for C-6 ($^2J_{CF}$ = 19.1 Hz) and C-7a ($^2J_{CF}$ = 21.0 Hz). Thus, the structures of the diastereoisomers were assigned as shown in Scheme 1. We have previously observed similar reactivity with Selectfluor reactions,[10] as have others with Selectfluor[45] and other related reagents.[46–52]

The reaction of Selectfluor with **3** afforded two mono-fluorinated structural isomers **9** (major) and **10** (minor), both with a molecular formula of $C_{17}H_{17}FO_6$ based on HRESIMS data. Comparison of the ^{1}H NMR data of **9** (Table S10) and **10** (Table S11) with those of **3** indicated the loss of one aromatic proton signal attributed to H-5 and H-7, respectively. In compound **9**, the C-4 methoxy resonance appeared more deshielded compared with the corresponding signal in **3** ($\Delta\delta$ 0.3), and showed a doublet splitting pattern due to a through space coupling with the fluorine at C-5 (Figs. S19–20). Unlike its chloro-analogue (**7**), this coupling was observed for the methoxy group at C-4 only, which suggested that, in the preferred conformer, the methoxy group at C6 in **9** is rotated away from the fluorine. Likewise, the methoxy groups in compound **10** showed no through-space coupling with the fluorine, indicated that the dominant conformation presents the C6 methoxy group away from the fluorine atom. Alternatively, compound **7** prefers to adopt a conformation where the methoxy group at C-6 is in close proximity to the fluorine due to the steric effect imposed by the chlorine atom.[53,54]

^{1}H NMR data for compound **9** also showed a doublet at δ 6.37 ($^3J_{HF}$ = 5.2 Hz), which was assigned to H-7 due to long-range coupling with fluorine (Figs. S19–S20). The correlation detected between the fluorine and C-5 (δ_C 139.6, doublet, $^1J_{CF}$ = 237.5 Hz) in the ^{19}F–^{13}C-HMQC data (Fig. S21) suggested the connection of fluorine to position 5. The attachment of fluorine at C-5 was further corroborated by the small doublet splitting observed for C-4 ($^2J_{CF}$ = 8.8 Hz) and C-6 ($^2J_{CF}$ = 11.3 Hz), establishing the structure of **9** as 5-fluoro-7-dechlorogriseofulvin. The structure of **10** was established in an analogous manner and was identified as 7-fluoro-7-dechlorogriseofulvin (Table S11; Figs. S24–S28), which was previously reported by Taub and co-workers.[35]

As was the case for **3**, reaction of compound **4** with Selectfluor yielded two mono-fluorinated structural isomers, **11** and **12**. The HRESIMS data served to verify the number of incorporated fluorine atoms in the compounds, while the NMR data was analyzed in the same manner as **9** (Tables S12–S13; Figs. S29–S38). This exercise established the structures of **11** and **12** as the 5′-OH analogues of compounds **9** and **10**, respectively.

2.3. Biological evaluation

Griseofulvin (**1**) and all 11 analogues (**2**–**12**) were evaluated for their cytotoxic activity against three different cancer cell lines, specifically MDA-MB-435, MDA-MB-231, and OVCAR3 (Tables 1 and S14). Compounds **1** and **10** had moderate to minimal cytotoxicity, with IC_{50} values ranging from approximately 6–50 μM, and other compounds were inactive at a 50 μM concentration. As a complementary dataset, we also tested **1**–**12** against human hepatoma Huh7.5.1 cells; the results were in agreement, indicating cytotoxic activity (ranging from approximately 10–25 μM) for **1** and **10** (Fig. S39).

All compounds (**1**–**12**) were also tested in an antifungal assay against *Microsporum gypseum*, a dermatophyte that causes tinea capitis, tinea corpus, and other fungal infections of the skin.[55,56] As shown in Tables 2 and S15, compound **10** retained the activity of **1**, while **7** showed a slight decrease in activity. Compound **10**

Table 1
Cytotoxicity results for the active compounds.[a] Compounds **2**–**9** and **11**–**12** were inactive (see Table S14).

Compound	IC_{50}		
	MDA-MB-435[c]	MDA-MB-231[d]	OVCAR3[e]
1	6.4 μM	*inactive*	48.5 μM
10	22.0 μM	*inactive*	*inactive*
Vinblastine[b]	0.5 nM	8.8 nM	1.8 nM

[a] A compound was indicated as *inactive* if no activity was observed at 50 μM.
[b] Positive control.
[c] Human melanoma cancer cells.
[d] Human breast cancer cells.
[e] Human ovarian cancer cells.

Table 2
Antifungal results against *Microsporum gypseum* for the active compounds.[a] Results for the other compounds in this study are shown in Table S15.

Compound	Zone of Inhibition (mm)[a]
1[b]	35 ± 1
7	23 ± 1
10	34 ± 1

[a] Mean diameter of inhibition zones at 25 μg/disk expressed as the mean of four replicates ± standard deviation.
[b] Positive control.

has previously been reported to retain the activity of **1** against the plant pathogen *Botrytis alii*,[35] but its activity against dermatophytes, particularly *M. gypseum*, has not been reported. The antifungal activity of **7** has not been reported previously.

2.4. Principal component analysis

The introduction of fluorine into molecules often results in significant changes in their molecular properties and biological activities.[30,57] The small atomic size, very high electronegativity, and low polarizability of the fluorine atom are just a few of the characteristics that can have important consequences in a lead optimization program, particularly one focused on modifying privileged scaffolds. To compare the distribution in chemical space between the natural analogues (**1**–**6**) versus the fluorinated analogues (**7**–**12**), and identify structural features important to maintain griseofulvin's cytotoxic and antifungal activities, principal component analysis (PCA) was performed. Eleven molecular properties that describe the electron distribution, molecular surface, and solubility of the compounds were used in an attempt to emphasize the variation given by the addition of a fluorine. The first two principal components (PC1, PC2) retrieved 68% of the covariance, whereas the first three principal components (PC1–PC3) retrieved 87% of the covariance. Interestingly, two electronic descriptors, namely electron affinity (EA (eV)) and electrotopological state (Estate), had the highest contribution to PC1, while QPlogS, a descriptor related to the solubility of the compounds, had the highest contribution to PC2. The dipole moment of the molecule, an electronic descriptor, had the highest contribution to PC3. These results further emphasized that the addition of a fluorine atom changed mostly the electronic distribution within the molecules, as reflected in the clear separation in the PCA of the fluorinated vs. non-fluorinated analogues of griseofulvin (Fig. 2).

The 3D representation of the chemical space of **1**–**12** revealed several interesting features (Fig. 2). For example, the 3D plot showed that the fungal metabolites clustered together, occupying a distinct region in the chemical space different from the fluorinated analogues, further illustrating that fluorine incorporation modified the molecular properties of the analogues. Additionally, fluorinated analogues **7**, **9**, and **10** were closer to griseofulvin in chemical space, suggesting that these analogues had similar electron distribution, solubility, and surface characteristics, which could indicate that these compounds had similar bioactivities. Similar results were observed on the 2D plot with PC1 and PC2 (Fig. S40). The association between chemical similarity (as visualized by PCA using the set of descriptors) and similarity in bioassay results held true for **7** and **10** but not for **9**. Compound **9** appears to be an activity cliff,[58] that is, a compound with similar structure to **1**, **7** and **10** but different biological activity. Further inspection of the structure of the molecules indicates that compound **9** lacks the halogen atom at the C-7 position. This suggests that the highly electronegative nature and geometric size of a halogen at C-7 of ring A appears to be an important feature of **1**, **7** and **10** in order to retain its biological effect. The biological activity observed for **7** can be rationalized given that the van der Waals radius of a fluorine atom (1.47 Å) is only slightly larger than that of hydrogen (1.20 Å). For compound **7**, the replacement of the hydrogen atom with a fluorine atom at C-5 did not impart a large change in molecular volume or the overall structure of the compound, thus

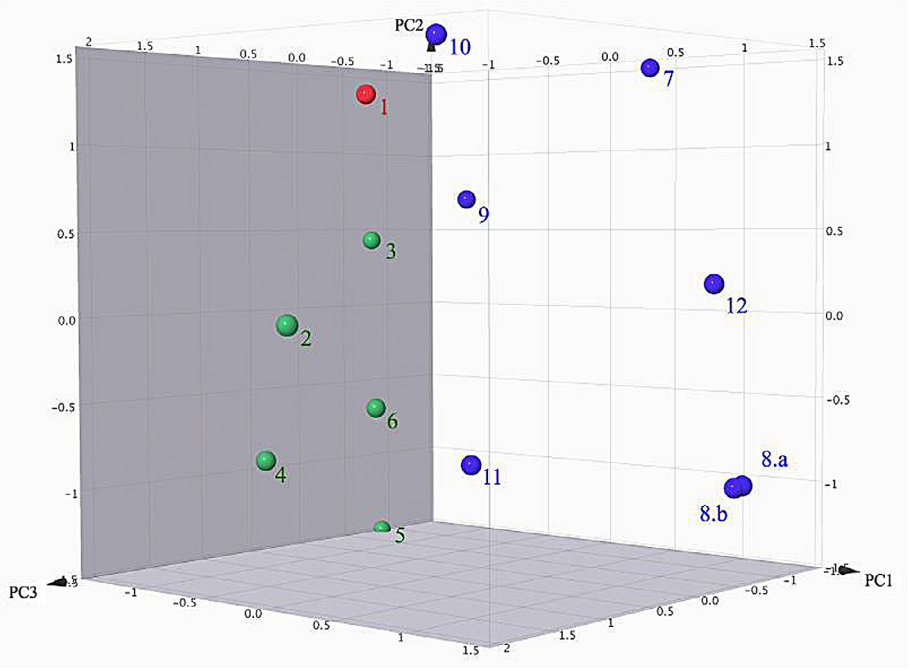

Fig. 2. Visual representation of the chemical space of griseofulvin (**1**, red), structurally related fungal analogues (**2**–**6**, green) and fluorinated semisynthetic derivatives (**7**–**12**, blue). This 3D plot was generated with the principal component analysis of 11 descriptors. The first three principal components recovered 87% of the covariance. The electron affinity (EA (eV)) and electrotopological state (Estate) had the highest contribution to the first principal component (PC1), while the predicted aqueous solubility (QPlogS) had the highest contribution to the second principal component (PC2). Dipole moment had the highest contribution to the third principal component (PC3).

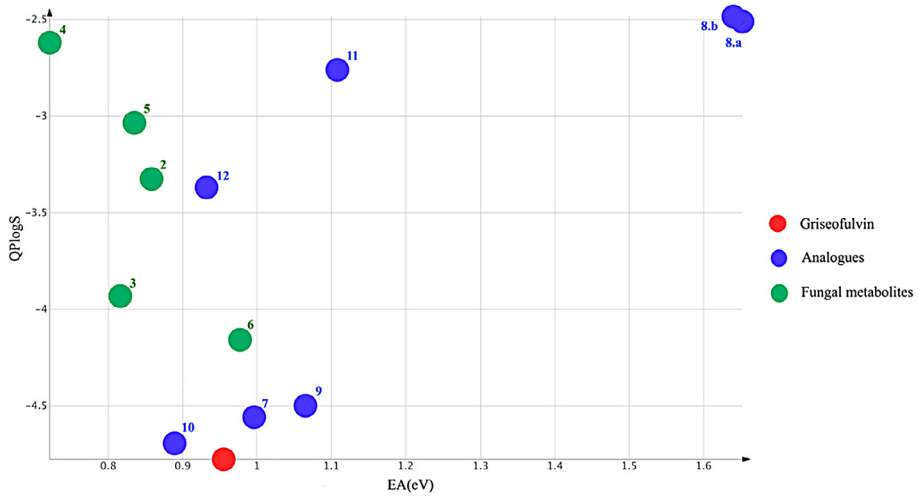

Fig. 3. A 2D visual representation of the chemical space of griseofulvin (**1**, red), structurally related fungal analogues (**2**–**6**, green) and fluorinated semisynthetic derivatives (**7**–**12**, blue) generated using two descriptors, predicted aqueous solubility (QPlogS; y-axis) and electron affinity [EA(Ev); x-axis].

retaining the antifungal activity. The properties of the chlorine atom, particularly at the C-7 position (ortho relative to the C-6 methoxy group), may also impart steric constraints and/or electrostatic effects that may be necessary for optimum molecular recognition between the compound and an active site/receptor. A fluorine atom at C-7, instead of chlorine, as was the case in compound **10**, may induce a similar electronic effect on the compound. The difference in electronegativity between the fluorine and carbon creates a large dipole moment in this bond, contributing to the overall electronic nature of the molecule, and this could lead to specific interactions with an active site/receptor. Although **10** retains the antifungal activity and cytotoxicity of **1**, a decrease in potency was observed, which may be explained by a decrease in the steric bulk in **10** at C-7 due to a difference in van der Waals radius between a fluorine atom (1.47 Å) and chlorine (1.75 Å).

A 2D plot of predicted aqueous solubility (QPlogS) and electron affinity (eV) similarly illustrated the variance in the distribution of the analogues across the chemical space (Fig. 3). The addition of fluorine to the griseofulvin analogues increased the electron affinity of the compounds, and this was manifested in chemical space as separating the fluorinated analogues from the natural secondary metabolites. Compound **7**, which is the C-5 fluorinated derivative of **1**, shared similar molecular properties in chemical space as **1**. Moreover, Figs. 2 and 3 illustrate that analogues **8a**/**8b**, which lost the aromaticity at ring A, were in a different region of chemical space, far from the rest of the analogues. It was observed that the fluorinative dearomatization of ring A in **8a**/**8b** significantly altered the properties of these compounds compared to griseofulvin (**1**). These changes could explain in part why **8a**/**8b** were inactive. Overall, the addition of fluorine or a hydroxy group to the A or C rings, respectively improved the predicted solubility (Fig. 3).

3. Conclusion

In summary, griseofulvin (**1**) and five analogues (**2**–**6**), with **4** being new to the literature, were isolated from *X. cubensis*. Additionally, a series of fluorinated analogues (**7**–**12**) were synthesized, each requiring only a single step from the isolated natural products using Selectfluor. The chemoselective nature of Selectfluor allowed for direct, site-specific mutation of the natural products without the use of protecting groups or other redox-modifications. Of the synthesized analogues, **8a**/**8b**, **9**, **11**, **12** are reported for the first time. All compounds were tested against the dermatophyte *M. gypseum* and in cytotoxicity assays against human melanoma cancer cells (MDA-MB-435), human breast cancer cells (MDA-MB-231), human ovarian cancer cells (OVCAR3), and human hepatoma cells (Huh7.5.1). Of the analogues, **10** retained the activity of **1** against *M. gypseum*, while **7** displayed decreased potency. Only compound **10** exhibited cytotoxic activity, but was less active compared to **1** against the MDA-MB-231 cells. To visualize the differences in the molecular and physicochemical properties generated by the addition of a single fluorine atom to the fungal secondary metabolites, PCA was used based on descriptors related to the electron distribution, solubility and molecular surface of the compounds. These descriptors captured the variation in the molecular properties and demonstrated that fluorinated analogues occupy a different region of chemical space than the fungal secondary metabolites. In addition, it was observed that the presence of a halogen in C-7 is important to maintain the biological activity for this class of compounds, as was observed for compounds **7** and **10**. These two compounds were close to griseofulvin in the chemical space, results that were consistent with the bioassay testing. This suggests that PCA can be a useful tool to visualize and guide the analysis of relevant structure-activity relationships. Taken together, these results demonstrate the synergistic opportunity of combining natural products chemistry, chemoselective semi-synthetic methods, and cheminformatics to rapidly develop and evaluate new, structurally-complex chemical entities from privilege scaffolds.

4. Experimental section

4.1. General experimental procedure

All solvents and chemicals were purchased from standard suppliers and were used without any further purification. The NMR data were collected using either a JEOL ECS-400 spectrometer (JEOL USA, Inc.) operating at 400 MHz for ^{1}H and 100 MHz for ^{13}C, and equipped with JEOL normal geometry broadband Royal probe; or a JEOL ECA-500 spectrometer (JEOL USA, Inc.) operating at 500 MHz for ^{1}H and 125 MHz for ^{13}C; or an Agilent 700 MHz NMR spectrometer (Agilent Technologies, Inc., Santa Clara, CA, USA) operating at 700 MHz for ^{1}H and 175 MHz for ^{13}C, and equipped with a cryoprobe. NMR chemical shift values were referenced to residual solvent signals for $CDCl_3$ (δ_H/δ_C 7.26/77.2). Data for ^{1}H NMR are reported as follows: chemical shift (δ ppm),

multiplicity (s = singlet, d = doublet, t = triplet, q = quartet, sept = septet, m = multiplet), coupling constant (Hz), and integration; whereas ^{13}C NMR analyses were reported in terms of chemical shift. HRESIMS data were obtained using a Thermo QExactive Plus mass spectrometer (ThermoFisher, San Jose, CA, USA) with an electrospray ionization source coupled with a Waters Acquity ultraperformance liquid chromatography (UPLC) system (Waters Corp.). The UPLC separation was performed using an Acquity BEH C_{18} column (50 mm × 2.1 mm i.d., 1.7 μm) equilibrated at 40 °C and a flow rate set at 0.3 mL/min. The mobile phase consisted of a linear CH_3CN/H_2O (acidified with 0.1% HCOOH) gradient starting at 15% CH_3CN to 100% CH_3CN over 8 min. The mobile phase was held for another 1.5 min at 100% CH_3CN before going back to the starting conditions. The HPLC separations were performed using Varian ProStar HPLC system connected to a ProStar 335 photodiode array detector (PDA) with UV detection set at 210 nm and 254 nm. Preparative reversed phase HPLC purification of samples was performed on a Phenomenex Gemini-NX C_{18} (5 μm; 250 × 21.2 mm) column using a 21 mL/min flow rate of the mobile phase consisting of a mixture of CH_3CN and H_2O (with 0.1% HCOOH). Flash column chromatography was carried out with a Teledyne ISCO Combiflash Rf connected to an ELSD and PDA detectors with UV detection set at 200–400 nm. Optical rotation data were acquired on a Rudolph Research Autopol III polarimeter (Rudolph Research Analytical, Flanders, NJ, USA). The UV data were acquired using a Varian Cary 100 Bio UV–Vis spectrophotometer (Varian Inc., Walnut Creek, CA, USA). The optical density (OD) at 600 nm was acquired using Thermo Scientific™ Genesys™ 20.

4.2. Fungal strain identification

Fungal strain MSX48662 was isolated from cedar wood collected in Little Rock, Arkansas and was identified using morphological and molecular methods[59] as described in detail previously.[31] Based on morphological characterization and molecular phylogenetic analysis, strain MSX48662 was identified as *Xylaria cubensis* (Sordariomycetes, Ascomycota). The sequence data for the strain utilized in the study was deposited in GenBank under accession number KX229783.

4.3. Fermentation, extraction, and isolation of natural products (**1**–**6**)

The fermentation of fungal strain MSX48662 was performed using procedures described previously with slight modifications.[60–62] Briefly, a fresh culture of the fungus was grown on a malt extract slant. Subsequently, a small agar plug with mycelium was inoculated in a liquid medium consisting of 2% soy peptone, 2% dextrose, and 1% yeast extract (YESD media). This was followed by incubation for approximately 7 days at room temperature (22 °C) with shaking. The seed culture was used to inoculate a Fernbach flask (2.8 L) containing rice (150 g) and H_2O (300 mL) and grown at rt for a period of 20 days.

The solid fermentation culture was extracted by addition of 1:1 $CH_3OH/CHCl_3$ (500 mL), followed by agitation for 16 h, and filtered. To the filtrate, 900 mL of $CHCl_3$ and 1500 mL of H_2O were added, and stirred for 30 min. The biphasic solution was partitioned, and the organic phase was collected and dried *in vacuo*. The resulting dried extract was further partitioned between CH_3OH/CH_3CN (1:1, 300 mL) and hexanes (300 mL) to obtain fractions weighing 2 g and 4 g, respectively. The CH_3OH/CH_3CN soluble partition was then adsorbed on Celite 545, and subjected to silica flash chromatography on a 24 g RediSep Rf Gold Si-gel column, eluting with use of a gradient solvent system of hexane/$CHCl_3$/CH_3OH at a flow rate of 35 mL/min over 71 column volumes for a duration of 68 min to give 100 fractions each containing 25 mL. The resulting fractions were then pooled according to their ELSD and UV profiles, which resulted to 16 subfractions.

Fraction 6 (230 mg) was subjected to preparative reversed-phase HPLC eluting with a linear gradient from 30% to 50% CH_3CN in H_2O (0.1% HCOOH) over 30 min to afford compound **1** (92 mg, t_R = 20.0 min), **2** (1.0 mg, t_R = 15.5 min), **3** (64 mg, t_R = 16.5 min), and **4** (15 mg, 12.5 min). Fraction 7 (115 mg) was purified using the same preparative HPLC conditions yielding more of compounds **2** (11 mg, t_R = 15.5 min) and **4** (17 mg, t_R = 12.5 min). Fraction 9 (250 mg) was similarly chromatographed but using a linear gradient from 20% to 40% CH_3CN in H_2O (0.1% HCOOH) over 15 min followed by an increase in the gradient to 80% CH_3CN to afford compounds **5** (1.9 mg, t_R = 17.0 min) and **6** (2.7 mg, t_R = 21.5 min).

4.3.1. (2*S*,6′*R*)-7-Chloro-2′,4,6-trimethoxy-6′-methyl-3*H*-spiro[benzofuran-2,1′-cyclohexan]-2′-ene-3,4′-dione; griseofulvin (**1**)

White solid; $[\alpha]_D^{27}$ +340 (*c* 0.1, $CHCl_3$); UV (MeOH) λ_{max} (log ε) 236 (4.4), 291 (4.4), 331 (3.7) nm; ^1H NMR (400 MHz, $CDCl_3$) δ = 0.96 (d, *J* = 6.8 Hz, 3H), 2.42 (dd, *J* = 16.8 Hz, 4.6 Hz, 1H), 2.84 (m, 1H), 3.03 (dd, *J* = 16.8 Hz, 13.4 Hz, 1H), 3.61 (s, 3H), 3.98 (s, 3H), 4.03 (s, 3H), 5.53 (s, 1H), 6.13 (s, 1H); ^{13}C NMR (100 MHz, $CDCl_3$) δ = 14.4, 36.5, 40.1, 56.5, 56.8, 57.1, 89.5, 90.9, 97.3, 105.0, 105.2, 157.9, 164.7, 169.6, 170.9, 192.6, 197.2 (See Table S2 and Fig. S1); HRESIMS *m*/*z* 353.0781 $[M+H]^+$ (calc'd for $C_{17}H_{18}ClO_6$, 353.0786).

4.3.2. (2*S*,5′*R*,6′*R*)-7-Chloro-5′-hydroxy-2′,4,6-trimethoxy-6′-methyl-3*H*-spiro[benzofuran-2,1′-cyclohexan]-2′-ene-3,4′-dione; 5′-hydroxygriseofulvin (**2**)

White solid; $[\alpha]_D^{27}$ +306 (*c* 0.1, MeOH); UV (MeOH) λ_{max} (log ε) 236 (4.2), 291 (4.2), 331 (3.6) nm; ^1H NMR (700 MHz, $CDCl_3$) δ = 1.11 (d, *J* = 6.7 Hz, 3H), 2.64 (dq, *J* = 12.2 Hz, 6.7 Hz, 1H), 3.65 (s, 3H), 3.99 (s, 3H), 4.04 (s, 3H), 4.68 (d, *J* = 12.2 Hz, 1H), 5.61 (s, 1H), 6.14 (s, 1H); ^{13}C NMR (175 MHz, $CDCl_3$) δ = 11.1, 43.6, 56.6, 57.1, 57.2, 71.5, 89.7, 91.2, 97.4, 101.8, 105.2, 158.0, 165.0, 169.8, 171.5, 192.6, 197.5 (See Table S3 and Fig. S2); HRESIMS *m*/*z* 369.0738 $[M+H]^+$ (calc'd for $C_{17}H_{18}ClO_7$, 369.0736).

4.3.3. (2*S*,6′*R*)-2′,4,6-Trimethoxy-6′-methyl-3*H*-spiro[benzofuran-2,1′-cyclohexan]-2′-ene-3,4′-dione; 7-dechlorogriseofulvin (**3**)

White solid; $[\alpha]_D^{27}$ +386 (*c* 0.1, MeOH); UV (MeOH) λ_{max} (log ε) 239 (4.4), 287 (4.4), 321 (3.8) nm; ^1H NMR (400 MHz, $CDCl_3$) δ = 0.94 (d, *J* = 6.6 Hz, 3H), 2.39 (dd, *J* = 16.8 Hz, 4.7 Hz, 1H), 2.74 (m, 1H), 3.03 (dd, *J* = 16.8 Hz, 13.4 Hz, 1H), 3.61 (s, 3H), 3.89 (s, 3H), 3.90 (s, 3H), 5.53 (s, 1H), 6.03 (d, *J* = 1.9 Hz, 1H), 6.23 (d, *J* = 1.9 Hz, 1H); ^{13}C NMR (100 MHz, $CDCl_3$) δ = 14.4, 36.7, 40.2, 56.2, 56.2, 56.8, 88.6, 90.0, 93.5, 104.4, 104.9, 159.2, 170.5, 171.5, 176.2, 192.7, 197.6 (Table S4 and Fig. S3); HRESIMS *m*/*z* 319.1175 $[M+H]^+$ (calc'd for $C_{17}H_{19}O_6$, 319.1176).

4.3.4. (2*S*,5′*R*,6′*R*)-5′-Hydroxy-2′,4,6-trimethoxy-6′-methyl-3*H*-spiro[benzofuran-2,1′-cyclohexan]-2′-ene-3,4′-dione; 7-dechloro-5′-hydroxygriseofulvin (**4**)

White solid; $[\alpha]_D^{27}$ +343 (*c* 0.1, MeOH); UV (solvent) λ_{max} (log ε) 230 (4.4), 288 (4.4), 321 (3.7) nm; ^1H NMR (400 MHz, $CDCl_3$) δ = 1.11 (d, *J* = 6.6 Hz, 3H), 2.55 (dq, *J* = 12.1 Hz, 6.6 Hz, 1H), 3.66 (s, 3H), 3.91 (s, 3H), 3.92 (s, 3H), 4.71 (d, *J* = 12.1 Hz, 1H), 5.61 (s, 1H), 6.06 (d, *J* = 1.1 Hz, 1H), 6.22 (d, *J* = 1.1 Hz, 1H); ^{13}C NMR (100 MHz, $CDCl_3$) δ = 11.2, 43.9, 56.3, 56.3, 57.1, 71.5, 88.6, 90.5, 93.7, 101.7, 104.4, 159.3, 170.8, 172.1, 176.3, 192.6, 197.8. (See Table S5 and Figs. S4–S6); HRESIMS *m*/*z* 335.1119 $[M+H]^+$ (calc'd for $C_{17}H_{19}O_7$, 335.1125).

*4.3.5. (2S,6′R)-6-Hydroxy-2′,4-dimethoxy-6′-methyl-3H-spiro [benzofuran-2,1′-cyclohexan]-2′-ene-3,4′-dione; 6-O-desmethyl-7-dechlorogriseofulvin (**5**)*

White solid; $[\alpha]_D^{27}$ +221 (*c* 0.1, MeOH); UV (solvent) λ_{max} (log ε) 248 (4.3), 290 (4.2), 322 (4.2) nm; ^{1}H NMR (400 MHz, $CDCl_3$) δ = 0.97 (d, 6.7 Hz, 3H), 2.43 (dd, *J* = 16.7 Hz, 4.8 Hz, 1H), 2.76 (dqd, *J* = 13.2 Hz, 6.7 Hz, 4.8 Hz, 1H), 3.08 (dd, *J* = 16.7 Hz, 13.2 Hz, 1H), 3.64 (s, 3H), 3.90 (s, 3H), 5.55 (s, 1H), 6.05 (d, *J* = 1.9 Hz, 1H), 6.20 (d, *J* = 1.9 Hz, 1H); ^{13}C NMR (100 MHz, $CDCl_3$) δ = 14.4, 36.7, 40.1, 56.3, 56.9, 90.0, 91.7, 93.6, 104.1, 104.7, 159.9, 167.9, 172.2, 175.8, 192.6, 198.4 (See Table S6 and Fig. S7); HRESIMS *m*/*z* 305.1032 $[M+H]^+$ (calc'd for $C_{16}H_{17}O_6$, 305.1020).

*4.3.6. (2S,6′R)-7-Chloro-6-hydroxy-2′,4-dimethoxy-6′-methyl-3H-spiro[benzofuran-2,1′-cyclohexan]-2′-ene-3,4′-dione; 6-O-desmethyl-7-griseofulvin (**6**)*

White solid; $[\alpha]_D^{27}$ +278 (*c* 0.1, MeOH); UV (solvent) λ_{max} (log ε) 243 (4.3), 288 (4.3), 347 (3.7) nm; ^{1}H NMR (400 MHz, $CDCl_3$) δ = 0.97 (d, *J* = 6.7 Hz, 3H), 2.44 (dd, *J* = 16.6 Hz, 4.7 Hz, 1H), 2.83 (dqd, *J* = 13.3 Hz, 6.7 Hz, 4.7 Hz, 1H), 3.04 (dd, *J* = 16.6 Hz, 13.3 Hz, 1H), 3.63 (s, 3H), 3.92 (s, 3H), 5.55 (s, 1H), 6.25 (s, 1H); ^{13}C NMR (100 MHz, $CDCl_3$) δ = 14.4, 36.5, 40.1, 56.6, 56.8, 91.2, 93.6, 95.2, 105.0, 105.4, 158.0, 161.8, 169.9, 170.7, 192.2, 197.2. (See Table S7 and Fig. S8); HRESIMS *m*/*z* 339.0646 $[M+H]^+$ (calc'd for $C_{16}H_{16}ClO_6$, 339.0630).

4.4. General fluorination procedure with Selectfluor

To an ice-cold acetonitrile solution of the natural product (0.02 M) was slowly added a freshly prepared acetonitrile solution of Selectfluor (0.02 M). The reaction mixture was allowed to stir at 0 °C for 4 h and then heated to 50 °C and monitored by HPLC. After 24 h, the reaction mixture was cooled to room temperature and the solvent was removed *in vacuo*.

*4.4.1. Fluorination of griseofulvin (**1**)*

Griseofulvin (**1**) (10.0 mg, 0.028 mmol) and Selectfluor (15.1 mg, 0.043 mmol) were reacted via the general method. The residue was purified by preparative HPLC eluting with a linear gradient from 40% to 60% CH_3CN in H_2O (0.1% HCOOH) over 30 min to obtain **7** (t_R = 19 min) and **8a**/**8b** (t_R = 13 min).

*4.4.1.1. (2S,6′R)-7-Chloro-5-fluoro-2′,4,6-trimethoxy-6′-methyl-3H-spiro[benzofuran-2,1′-cyclohexan]-2′-ene-3,4′-dione; 5-Fluorogriseofulvin (**7**).* White solid; $[\alpha]_D^{27}$ +290 (*c* 0.1, MeOH); 1.0 mg (10% yield); white solid; ^{1}H NMR (400 MHz, $CDCl_3$) δ = 0.95 (d, *J* = 6.7 Hz, 3H), 2.45 (dd, *J* = 16.7 Hz, 4.4 Hz, 1H), 2.85 (dqd, *J* = 13.3 Hz, 6.7 Hz, 4.4 Hz, 1H), 2.98 (dd, *J* = 16.7 Hz, 13.3 Hz, 1H), 3.64 (s, 3H), 4.17 (d, *J* = 3.1 Hz, 3H), 4.20 (d, *J* = 3.1 Hz, 3H), 5.56 (s, 1H). ^{13}C NMR (100 MHz, $CDCl_3$) δ = 14.4, 36.6, 40.0, 56.9, 62.1 (d, *J* = 7.0 Hz), 62.6 (d, *J* = 6.0 Hz), 90.6, 103.4, 105.2, 108.0, 142.9 (d, *J* = 244.3 Hz), 144.7 (d, *J* = 9.0 Hz), 153.9 (d, *J* = 12.1 Hz), 164.9, 170.5, 193.5 (d, *J* = 4.0 Hz), 196.8. ^{19}F NMR (470 MHz, $CDCl_3$) δ = −155.5 (sept. *J* = 3.1 Hz) (See Table S8 and Figs. S9–S13); HRESIMS *m*/*z* 371.0696 $[M+H]^+$ (calc'd for $C_{17}H_{17}ClFO_6$ 371.0692).

*4.4.1.2. (2S,6′R)-7-Chloro-5-fluoro-2′,4,6-trimethoxy-6′-methyl-3H-spiro[benzofuran-2,1′-cyclohexan]-2′-ene-3,4′-dione (**8a**/**8b**).* Glassy yellow; 2.3 mg (Isolated as a diastereoisomeric mixture of the two compounds with a 2:1 ratio) $[\alpha]_D^{27}$ +194 (*c* 0.1, MeOH) (23% yield); **8a**:^{1}H NMR (400 MHz, $CDCl_3$) δ = 1.00 (d, *J* = 6.3 Hz, 3H), 2.46 (dd, *J* = 16.1 Hz, 4.2 Hz, 1H), 2.89 (m, 1H), 2.97 (m, 1H), 3.69 (s, 3H), 3.94 (s, 3H), 5.55 (d, *J* = 1.8 Hz, 1H), 5.58 (s, 1H). ^{13}C NMR (100 MHz, $CDCl_3$) δ = 14.1, 36.1, 39.7, 57.1, 57.8, 94.1, 94.1 (d, *J* = 252.3), 102.0 (d, *J* = 2.0 Hz), 105.4, 110.1 (d, *J* = 3.0 Hz), 162.8 (d, *J* = 19.1 Hz), 168.1, 176.9 (d, *J* = 2.0 Hz), 185.3 (d, *J* = 21.0 Hz), 191.8, 195.8. ^{19}F NMR (470 MHz, $CDCl_3$) δ = −126.4 (d, *J* = 1.8 Hz). **8b**: ^{1}H NMR (400 MHz, $CDCl_3$) δ = 1.06 (d, *J* = 6.3 Hz, 3H), 2.46 (dd, *J* = 16.1 Hz, 4.2 Hz, 1H), 2.95 (m, 1H), 2.97 (m, 1H), 3.67 (s, 3H), 3.94 (s, 3H), 5.55 (d, *J* = 1.8 Hz, 1H), 5.58 (s, 1H). ^{13}C NMR (100 MHz, $CDCl_3$) δ = 14.1, 36.5, 39.7, 57.2, 57.8, 94.0 (d, *J* = 254.3), 94.1, 102.0 (d, *J* = 2.0 Hz), 105.5, 110.0 (d, *J* = 3.0 Hz), 162.8 (d, *J* = 19.1 Hz), 167.7, 176.9 (d, *J* = 2.0 Hz), 185.4 (d, *J* = 21.0 Hz), 191.7, 195.8. ^{19}F NMR (470 MHz, $CDCl_3$) δ = −127.5 (d, *J* = 1.8 Hz) (See Table S9 and Figs. S14–S18); HRESIMS *m*/*z* 357.0543 $[M+H]^+$ (calc'd for $C_{16}H_{15}ClFO_6$ 357.0536).

*4.4.2. Fluorination of 7-dechlorogriseofulvin (**3**)*

7-Dechlorogriseofulvin (**3**) (7.0 mg, 0.022 mmol) and Selectfluor (11.7 mg, 0.033 mmol) were reacted via the general method. The residue was purified by preparative HPLC eluting with a linear gradient from 30% to 50% CH_3CN in H_2O (0.1% HCOOH) over 30 min to obtain compounds **9** (t_R = 21 min), and **10** (t_R = 18 min).

*4.4.2.1. (2S,6′R)-5-Fluoro-2′,4,6-trimethoxy-6′-methyl-3H-spiro[benzofuran-2,1′-cyclohexan]-2′-ene-3,4′-dione; 5-Fluoro-7-dechlorogriseofulvin (**9**).* White solid; $[\alpha]_D^{27}$ +289 (*c* 0.1, MeOH); 2.3 mg (33% yield); ^{1}H NMR (500 MHz, $CDCl_3$) δ = 0.95 (d, *J* = 6.9 Hz, 3H), 2.75 (dd, *J* = 17.2 Hz, 4.6 Hz, 1H), 2.75 (m, 1H), 3.02 (dd, *J* = 17.2 Hz, 13.2 Hz, 1H), 3.63 (s, 3H), 3.98 (s, 3H), 4.20 (d, *J* = 3.3 Hz, 3H), 5.55 (s, 1H), 6.37 (d, *J* = 5.2 Hz, 1H). ^{13}C NMR (125 MHz, $CDCl_3$) δ = 14.4, 36.7, 40.1, 56.8, 57.0, 62.1 (d, *J* = 7.5 Hz), 89.8, 90.0, 105.0, 105.5, 139.6 (d, *J* = 237.5 Hz), 145.0 (d, *J* = 8.8 Hz), 158.6 (d, *J* = 11.3 Hz), 170.4, 171.1, 193.4, 197.2. ^{19}F NMR (470 MHz, $CDCl_3$) δ = −163.0 (m) (See Table S10 and Fig. 19–23); HRESIMS *m*/*z* 337.1080 $[M+H]^+$ (calc'd for $C_{17}H_{18}FO_6$ 337.1082).

*4.4.2.2. (2S,6′R)-7-Fluoro-2′,4,6-trimethoxy-6′-methyl-3H-spiro[benzofuran-2,1′-cyclohexan]-2′-ene-3,4′-dione; 7-Fluoro-7-dechlorogriseofulvin (**10**).* White solid; $[\alpha]_D^{27}$ +230 (*c* 0.1, MeOH); 1.3 mg (19% yield); ^{1}H NMR (700 MHz, $CDCl_3$) δ = 0.98 (d, *J* = 6.7 Hz, 3H), 2.43 (dd, *J* = 17.2 Hz, 4.8 Hz, 1H), 2.81 (m, 1H), 3.03 (dd, *J* = 17.2 Hz, 13.4 Hz, 1H), 3.62 (s, 3H), 3.95 (s, 3H), 4.02 (s, 3H), 5.54 (s, 1H), 6.09 (d, *J* = 5.2 Hz, 1H). ^{13}C NMR (175 MHz, $CDCl_3$) δ = 14.4, 36.6, 40.2, 56.5, 56.8, 57.3, 90.1, 91.0, 105.0, 105.0, 132.4 (d, *J* = 238.0 Hz), 154.7 (d, *J* = 1.8 Hz), 157.4 (d, *J* = 7.0 Hz), 160.3 (d, *J* = 8.8 Hz), 170.9, 192.4 (d, *J* = 2.4 Hz), 197.1. ^{19}F NMR (470 MHz, $CDCl_3$) δ = −171.3 (d, *J* = 5.2 Hz) (See Table S11 and Figs. S24–S28); HRESIMS *m*/*z* 337.1079 $[M+H]^+$ (calc'd for $C_{17}H_{18}FO_6$ 337.1082).

*4.4.3. Fluorination of 7-dechloro-5′-hydroxygriseofulvin (**4**)*

7-Dechloro-5′-hydroxygriseofulvin (**4**) (6.2 mg, 0.018 mmol) and Selectfluor (9.8 mg, 0.027 mmol) were reacted via the general method. After purification using preparative HPLC eluting with a linear gradient from 30% to 50% CH_3CN in H_2O (0.1% HCOOH) over 30 min to obtain compounds **11** (t_R = 16 min), and **12** (t_R = 14 min).

*4.4.3.1. (2S,5′R,6′R)-5-Fluoro-5′-hydroxy-2′,4,6-trimethoxy-6′-methyl-3H-spiro[benzofuran-2,1′-cyclohexan]-2′-ene-3,4′-dione; 5-Fluoro-5′-hydroxy-7-dechlorogriseofulvin (**11**).* White solid; $[\alpha]_D^{27}$ +240 (*c* 0.05, MeOH); 1.7 mg (27% yield); ^{1}H NMR (700 MHz, $CDCl_3$) δ = 1.10 (d, *J* = 6.9 Hz, 3H), 2.54 (dq, *J* = 12.0 Hz, 6.9 Hz, 1H), 3.67 (s, 3H), 3.98 (s, 3H), 4.21 (d, *J* = 3.6 Hz, 3H), 4.67 (d, *J* = 12.0 Hz, 1H), 5.61 (s, 1H), 6.36 (d, *J* = 5.4 Hz, 1H). ^{13}C NMR (175 MHz, $CDCl_3$) δ = 11.1, 43.7, 57.1, 57.1, 62.1 (d, *J* = 6.7 Hz), 71.4, 89.1, 90.4, 101.9, 105.5 (d, *J* = 1.4 Hz), 139.6 (d, *J* = 241.6 Hz), 145.1 (d, *J* = 7.9 Hz), 158.9 (d, *J* = 11.2 Hz), 170.5, 171.7, 193.4 (d, *J* = 3.3 Hz), 197.5. ^{19}F NMR (470 MHz, $CDCl_3$) δ = −162.7 (dq, *J* = 5.4 Hz, 3.6 Hz)

(See Table S12 and Figs. S29–S33); HRESIMS *m/z* 353.1027 $[M+H]^+$ (calc'd for $C_{17}H_{18}FO_7$ 353.1031).

*4.4.3.2. (2S,5′R,6′R)-7-Fluoro-5′-hydroxy-2′,4,6-trimethoxy-6′-methyl-3H-spiro[benzofuran-2,1′-cyclohexan]-2′-ene-3,4′-dione; 7-Fluoro-5′-hydroxy-7-dechlorogriseofulvin (**12**).* White solid; $[\alpha]_D^{27}$ +270 (*c* 0.03, MeOH); 1.0 mg (16% yield); ^{1}H NMR (700 MHz, $CDCl_3$) δ = 1.13 (d, *J* = 6.3 Hz, 3H), 2.60 (dq, *J* = 12.0 Hz, 6.3 Hz, 1H), 3.66 (s, 3H), 3.95 (s, 3H), 4.03 (s, 3H), 4.68 (d, *J* = 12.0 Hz, 1H), 5.61 (s, 1H), 6.10 (d, *J* = 5.1 Hz, 1H); ^{13}C NMR (175 MHz, $CDCl_3$) δ = 11.1, 43.7, 56.6, 57.1, 57.3, 71.4, 90.2, 91.2, 101.8, 104.9, 132.2 (d, *J* = 237.0 Hz), 154.8 (d, *J* = 1.8 Hz), 157.6 (d, *J* = 8.8 Hz), 160.3 (d, *J* = 10.5 Hz), 171.5, 192.4 (d, *J* = 2.7 Hz), 197.4. ^{19}F NMR (470 MHz, $CDCl_3$) δ = −171.1 (d, *J* = 5.1 Hz) (See Table S13 and Figs. S34–38); HRESIMS *m/z* 353.1022 $[M+H]^+$ (calc'd for $C_{17}H_{18}FO_7$ 353.1031).

4.5. Cytotoxicity assay

Human melanoma cancer cells (MDA-MB-435), human breast cancer cells (MDA-MB-231) and human cancer cells (OVCAR3) were procured from the American Type Culture Collection (Manassas, VA). The cell lines were cultivated in RPMI 1640 medium, supplemented with fetal bovine serum (10%), penicillin (100 units/mL), and streptomycin (100 μg/mL); and grown at 37 °C under 5% CO_2. Huh7.5.1 cells were cultured in DMEM medium as previously described.[63] Cells in log-phase growth were harvested by trypsinization followed by two washing to remove all traces of enzyme. Cells were seeded in 96-well clear, flat-bottom plate (Corning) at a density of 5000 cells per well, and each plate was incubated overnight at 37 °C under 5% CO_2. Samples dissolved in DMSO were diluted and added to the appropriate wells to give final concentrations of 20 and 2 μg/mL (20, 4, 0.8, 0.16, and 0.032 μM for pure compounds) with a total volume of 100 μL and 0.5% DMSO. The cells with the test samples were then incubated for 72 h at 37 °C. Cell viability was examined using a commercial absorbance assay (Cell titer 96® Aqueous One Solution Cell Proliferation Assay, Promega Corp, Madison, WI). For Huh7.5.1 cells, viability was determined by measuring ATP levels in cells using the ATPlite kit (Perkin Elmer, Waltham, MA) as previously described.[64] Results are expressed as percent survival relative to the solvent (DMSO) control.

4.6. Antifungal assay

The test fungal isolate *Microsporum gypseum* was kept at the Fungal Culture Collection at the Department of Chemistry and Biochemistry at the University of North Carolina at Greensboro. The test isolate was maintained on Saboraud dextrose agar plates at rt and sub-cultured monthly throughout this study. The test compounds were dissolved in DMSO and 5 μL were loaded onto a 6 mm filter paper disk to obtain the desired 25 μg sample concentration per disk. Antimycotic activity was carried out by the agar disk diffusion method.[65,66] Following growth of the fungi, the conidia were harvested in sterile distilled deionized water. The inoculum was adjusted to 0.5–1.0 OD ($\sim 10^5$ cells/mL) at 600 nm. Mueller-Hinton agar supplemented with 2% glucose and 0.5 μg/ml methylene blue was then seeded with 100 μL of the inoculum. Disks impregnated with the test agent were aseptically added onto the surface of the inoculated plates. The sensitivity of the microorganism to the compounds was determined after 5 d by measuring the diameter (in mm) of the zones of inhibition around the disks.

4.7. Principal component analysis

The structures and SMILES where generated with ChemDraw and 11 molecular properties were calculated using QikProp (version 3.5).[67] The calculated properties can be divided in three main groups: electronic, surface, and solubility descriptors. The electronic descriptors were: calculated electron affinity EA (eV), predicted polarizability (QPpolrz), electrotopological state (Estate) and dipole moment of the molecule (dipole). The surface descriptors were: total solvent accessible area (SAS), hydrophilic component of the SASA (FISA), carbon and attached hydrogen component of the SASA (PISA), Van der Waals surface area of polar nitrogen and oxygen atoms (PSA), and solvent-accessible surface area of fluorine atoms (SAFluorine). The solubility descriptors were: free energy of solvation in hexadecane (QPlogPC16) and predicted aqueous solubility (QPlogS). To generate a visual representation of the chemical space based on these properties, a principal component analysis was performed using Molecular Operating Environment (version 2014.08),[68] and Data Warrior (version 4.2.2).[69]

Acknowledgments

This research was supported via program project grant P01 CA125066 from the National Cancer Institute/National Institutes of Health, Bethesda, MD, USA. The high-resolution mass spectrometry data were acquired in the Triad Mass Spectrometry Laboratory at the University of North Carolina at Greensboro, Greensboro, NC, USA. We also acknowledge the support of the Universidad Nacional Autónoma de México (UNAM), grant PAPIME PE200116, and the Programa de Apoyo a la Investigación y el Posgrado (PAIP), grant 5000-9163, Facultad de Química, UNAM. The authors thank Dr. José Rivera-Chávez (UNCG) and Oscar Palomino-Hernández (UNAM) for helpful suggestions.

A. Supplementary data

Supplementary data associated with this article can be found, in the online version, at http://dx.doi.org/10.1016/j.bmc.2017.07.041.

References

1. Harvey AL, Clark RL, Mackay SP, Johnston BF. *Expert Opin Drug Discov*. 2010;5:559–568.
2. Ganesan A. *Curr Opin Chem Biol*. 2008;12:306–317.
3. Evans BE, Rittle KE, Bock MG, et al. *J Med Chem*. 1988;31:2235–2246.
4. Nicolaou KC, Pfefferkorn JA, Roecker AJ, Cao GQ, Barluenga S, Mitchell HJ. *J Am Chem Soc*. 2000;122:9939–9953.
5. Newman DJ, Cragg GM. *J Nat Prod*. 2012;75:311–335.
6. Newman DJ, Cragg GM. *J Nat Prod*. 2016;79:629–661.
7. El-Elimat T, Zhang X, Jarjoura D, et al. *ACS Med Chem Lett*. 2012;3:645–649.
8. González-Medina M, Prieto-Martínez FD, Naveja JJ, et al. *Future Med Chem*. 2016;8:1399–1412.
9. González-Medina M, Owen J, El-Elimat T, et al. *Front Pharmacol*. 2017;8.
10. Fakhouri L, El-Elimat T, Hurst DP, et al. *Bioorg Med Chem*. 2015;23:6993–6999.
11. Ayers S, Graf TN, Adcock AF, et al. *J Nat Prod*. 2011;74:1126–1131.
12. Huang DB, Ostrosky-Zeichner L, Wu JJ, Pang KR, Tyring SK. *Dermatol Ther*. 2004;17:517–522.
13. Petersen AB, Rønnest MH, Larsen TO, Clausen MH. *Chem Rev*. 2014;114:12088–12107.
14. Di Santo R. *Nat Prod Rep*. 2010;27:1084–1098.
15. Gentles JC. *Nature*. 1958;182:476–477.
16. Oxford AE, Raistrick H, Simonart P. *Biochem J*. 1939;33:240–248.
17. Raab MS, Breitkreutz I, Anderhub S, et al. *Cancer Res*. 2012;72:5374–5385.
18. Ho YS, Duh JS, Jeng JH, et al. *Int J Cancer*. 2001;91:393–401.
19. Mauro V, Carette D, Pontier-Bres R, et al. *Apoptosis*. 2013;18:480–491.
20. Rebacz B, Larsen TO, Clausen MH, et al. *Cancer Res*. 2007;67:6342–6350.
21. Rathinasamy K, Jindal B, Asthana J, Singh P, Balaji PV, Panda D. *BMC Cancer*. 2010;10:213.
22. Rønnest MH, Raab MS, Anderhub S, et al. *J Med Chem*. 2012;55:652–660.
23. Singh P, Rathinasamy K, Mohan R, Panda D. *IUBMB Life*. 2008;60:368–375.
24. Pasquier E, Kavallaris M. *IUBMB Life*. 2008;60:165–170.
25. Dumontet C, Jordan MA. *Nat Rev Drug Discov*. 2010;9:790–803.
26. Zomorodian K, Uthman U, Tarazooie B, Rezaie S. *J Infect Chemother*. 2007;13:373–379.
27. Wang J, Sanchez-Rosello M, Acena JL, et al. *Chem Rev*. 2014;114:2432–2506.
28. Zhou P, Zou J, Tian F, Shang Z. *J Chem Inf Model*. 2009;49:2344–2355.

29. Zhou Y, Wang J, Gu Z, et al. *Chem Rev*. 2016;116:422–518.
30. Isanbor C, O'Hagan D. *J Fluorine Chem*. 2006;127:303–319.
31. Brooks WC, Paguigan ND, Raja HA, et al. *Magn Reson Chem*. 2016. http://dx.doi.org/10.1002/mrc.4571.
32. Zhong J, Gastaminza P, Cheng G, et al. *Proc Natl Acad Sci USA*. 2005;102:9294–9299.
33. Townley ER. Griseofulvin. In: KlausFlorey F, ed. *Analytical Profiles of Drug Substances*. Academic Press; 1979:219–249.
34. Chooi Y-H, Cacho R, Tang Y. *Chem Biol*. 2010;17:483–494.
35. Taub D, Kuo CH, Wendler NL. *J Org Chem*. 1963;28:2752–2755.
36. Barton DHR, Hesse RH, Ogunkoya L, Westcott ND, Pechet MM. *J Chem Soc, Perkin Trans 1*. 1972;2889–2891.
37. Barton DHR, Ganguly AK, Hesse RH, Loo SN, Pechet MM. *Chem Commun (London)*. 1968;806–808.
38. Schack CJ, Christe KO. *Inorg Chem*. 1979;18:2619–2620.
39. Barton DHR, Godinho LS, Hesse RH, Pechet MM. *Chem. Commun. (London)*. 1968;804–806.
40. Nyffeler PT, Duron SG, Burkart MD, Vincent SP, Wong CH. *Angew Chem Int Ed Engl*. 2005;44:192–212.
41. Woodhead AJ, Angove H, Carr MG, et al. *J Med Chem*. 2010;53:5956–5969.
42. Singh RP, Shreeve JNM. *Acc Chem Res*. 2004;37:31–44.
43. Hierso J-C. *Chem Rev*. 2014;114:4838–4867.
44. Weigert FJ, Roberts JD. *J Am Chem Soc*. 1971;93:2361–2369.
45. Stavber S, Jereb M, Zupan M. *Synlett*. 1999;1999:1375–1378.
46. Fukuhara T, Akiyama Y, Yoneda N, Tada T, Hara S. *Tetrahedron Lett*. 2002;43:6583–6585.
47. Meurs JHH, Sopher DW, Eilenberg W. *Angew Chem*. 1989;101:955–956.
48. Norihiko Y, Tsuyoshi F. *Chem Lett*. 2001;30:222–223.
49. Karam O, Martin-Mingot A, Jouannetaud M-P, Jacquesy J-C, Cousson A. *Tetrahedron*. 2004;60:6629–6638.
50. Kovtonyuk VN, Kobrina LS, Yakobson GG. *J Fluorine Chem*. 1985;28:89–98.
51. Gao Z, Lim YH, Tredwell M, et al. *Angew Chem Int Ed*. 2012;51:6733–6737.
52. Soelch RR, Mauer GW, Lemal DM. *J Org Chem*. 1985;50:5845–5852.
53. Holl MG, Struble MD, Siegler MA, Lectka T. *J Fluorine Chem*. 2016;188:126–130.
54. Naumann K. *Pest Manag Sci*. 2000;56:3–21.
55. Singh CJ. *Mycoses*. 2011;54:e183–e188.
56. Achterman RR, Smith AR, Oliver BG, White TC. *Fungal Genet Biol*. 2011;48:335–341.
57. Gillis EP, Eastman KJ, Hill MD, Donnelly DJ, Meanwell NA. *J Med Chem*. 2015;58:8315–8359.
58. Medina-Franco JL. *Chem Biol Drug Des*. 2013;81:553–556.
59. Raja HA, Miller AN, Pearce CJ, Oberlies NH. *J Nat Prod*. 2017;80:756–770.
60. El-Elimat T, Figueroa M, Raja HA, et al. *Eur J Org Chem*. 2015;2015:109–121.
61. Figueroa M, Graf TN, Ayers S, et al. *Antibiot.*. 2012;65:559–564.
62. Kaur A, Raja HA, Darveaux BA, et al. *Magn Reson Chem*. 2015;53:616–619.
63. Polyak SJ, Morishima C, Lohmann V, et al. *Proc Natl Acad Sci USA*. 2010;107:5995–5999.
64. Lovelace ES, Wagoner J, MacDonald J, et al. *J Nat Prod*. 2015;78:1990–2000.
65. Balouiri M, Sadiki M, Ibnsouda SK. *J Pharm Anal*. 2016;6:71–79.
66. Nweze EI, Mukherjee PK, Ghannoum MA. *J Clin Microbiol*. 2010;48:3750–3752.
67. *QikProp, version 3.5*. New York, NY: Schrödinger, LLC; 2012 www.schrodinger.com.
68. Molecular operating environment (MOE), version 2014.08, Chemical Computing Group Inc., Montreal, Quebec, Canada. www.chemcomp.com.
69. Sander T, Freyss J, von Korff M, Rufener C. *J Chem Inf Model*. 2015;55:460–473.